Exploring the Leakage Inductance of Transformers Used in Dual Active Bridge

Denisse A. Meza Soria, *Student Member, IEEE*, Satish Ranade, *Senior Member, IEEE*, Olga Lavrova, *Member, IEEE*
Klipsch School of Electrical and Computer Engineering
New Mexico State University
Las Cruces, USA

***Abstract*—Battery Energy Storage Systems (BESS) are critical to achieving reliability and efficiency in the modern electric grid. Dual Active Bridges (DAB) are often proposed for such integration since they can allow multiple sources and electrical isolation via a high-frequency transformer. In defined applications, DABs rely on the magnetizing and leakage inductance of their high-frequency transformers to achieve their performance requirement. In this paper, the inductance parameters of two types of two-winding transformers are investigated using the Finite Element Analysis (FEA) software ANSYS Maxwell. The variation of the inductance values due to the windings' distribution and core geometry was studied by establishing a parametric analysis. Prototypes were built and tested to compare the inductances actual measurements versus the simulation results. Exploring the possibility of characterizing the inductances of a transformer from a simulation standpoint is of interest in order to construct customized transformers with the optimal characteristic required in a specific DAB design.**

***Index Terms*--dual-active bridge, FEA simulation, inductance, renewable energy integration, transformers.**

I. INTRODUCTION

The addition of renewable energy systems to the traditional grid is desirable to meet the increasing power demand with clean energy, keeping the grid stable, and improving its resiliency. Due to the variability of power generation in renewable energy sources, the integration to the grid is a challenge. However, Energy Storage Systems (ESS) can be the solution to find an equilibrium between the variation of renewable generation and the actual power demand. For this, the optimization of Power Conversion Systems (PCS) is essential to improve reliability and feasibility of deployments of Battery Energy Storage Systems (BESS). The use of High-Frequency Transformers (HFT) for PCS is advantageous over traditional transformers because of their smaller size, lightweight, and saturation point. Authors agree that Dual Active Bridge (DAB) converters lead the way to improve DC-DC regulation in BESS [1]-[3]. In [4], the authors describe the process of designing an optimal DAB converter with Phase Shift Modulation (PSM) as a control strategy. They find that the leakage inductance of the HFT is one of the primary parameters for achieving the voltage and power specification required. Thus, the characterization of inductance in transformer designs is important to facilitate the customizing of inductance parameters.

This paper presents the analysis of the variation of inductance parameters in transformers for power electronics as affected by core geometry, separation of turns and winding distribution. In two selected transformer core geometries, a toroidal and an EE core, Ansys Maxwell Finite Element Analysis (FEA) simulation was used to find the electromagnetic solution and derive the inductance parameters of the transformers.

The methodology used to derive the inductance parameters is provided in Section II. Section III describes the simulation cases selected. In section IV, the validation of the prototypes is presented, and the results are summarized in Section V. Lastly, Section VI presents the conclusions.

II. THEORETICAL FRAMEWORK

This section describes the initial analysis of the transformer model and the derivation of the leakage inductance, following with a brief description of the ANSYS Maxwell solution approach to find the inductance parameters using a magnetostatic analysis.

A. Transformer Model

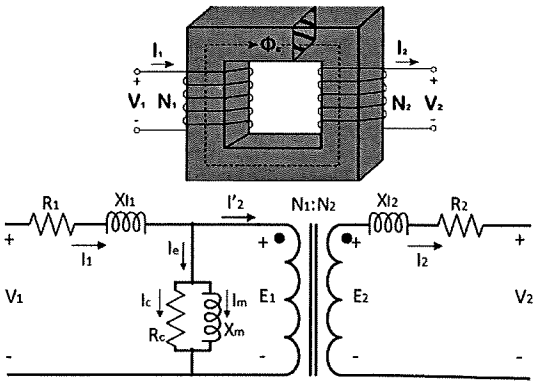

Figure 1. Practical transformer model.

978-1-7281-0407-2/19/$31.00 ©2019 IEEE

and it generates an inductance matrix that contains the nominal self-inductances and mutual inductances of the coils in the model. Since the magnetostatic solution finds the flux lines in the whole solution space; the inductance matrix obtained by ANSYS Maxwell does account for the leakage inductance within the self-inductance component of each corresponding current source.

III. ANSYS MAXWELL SIMULATION OF PROTOTYPES

In this section, two FEA simulations are presented. A different winding distribution was assigned to the toroidal core and EE core transformers. Both transformers have primary and secondary windings made of the AWG 22 bare copper wire, and the numbers of turns are 6 and 18 turns respectively. The starting separation distance between the turns and the core is set to 0.5 mm, and the excitation current in the primary is set to 25 *mA*. Since the application of the transformers is intended to be low power conversion systems, the core operation point is assumed to be located in the linear area of the B-H curve. Therefore, the relative permeability is considered constant in both transformers. The parametric analysis focused on the sweep of variables such as the distance between turns of each winding and the spacing between overlapping windings.

A. Simulation of Toroidal Core Transformer

The magnetic core dimensions can be seen in Fig. 3, and a summary of the geometric dimensions and characteristics is provided in Table I.

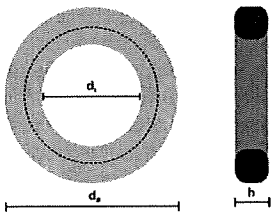

Figure 3. Toroidal core dimensions diagram.

TABLE I. TOROIDAL CORE DIMENSIONS AND CHARACTERISTICS

Dimensions and Characteristics		Value
Outside diameter[a]	d_o	34.0 mm
Inside diameter[a]	d_i	20.5 mm
Core height[a]	h	10.0 mm
Initial permeability[a]	μ_i	4300 H/m
Effective length[a]	l_e	82.06 mm
Effective cross-section area[a]	A_e	66.08 mm^2
Inductance factor[a] (A_L=L/N^2)	A_L	4360 nH/ N^2

a. Extracted from [11].

In a toroidal transformer, the windings can be distributed in many ways. Each winding distribution design modifies the leakage inductance of the transformer allowing to make adjustments to obtain a desired inductance value. Some of the geometry values that can be purposely varied are the distance between the primary and the core, the distance between windings, and the position of the windings in the core circumference with and without overlapping them. Further configuration cases and their results can be found in [12]. In this paper, the example presented corresponds to a design with a non-overlapping distribution with increments in the distance between the turns of each winding.

As shown in Fig. 4, the coils in the transformer are located 180° apart, and each winding covers a quarter of the toroidal core circumference. The parametric analysis redistributes the coils starting from 90° of core coverage to 180°. In other words, the distance between turns in each coil was increased gradually until the coil spread over half the toroidal core in a 180° sector as maximum.

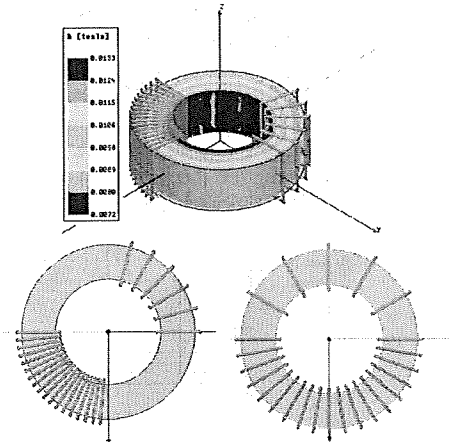

Figure 4. Toroidal core transformer simulation.

B. Simulation of EE Core Transformer

A magnetostatic simulation was executed for an EE shell-type core transformer. In this design, the windings are placed in the inner leg of the core. Fig. 5 illustrates the geometry and dimensions of the E core selected to form the EE core, and Table II summarizes the characteristics and dimensions of this piece.

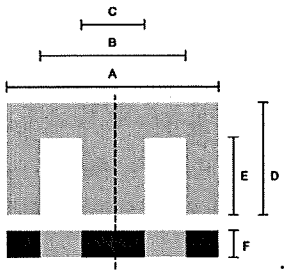

Figure 5. EE core dimensions diagram.

TABLE II. EE CORE DIMENSIONS AND CHARACTERISTICS

Dimensions and Characteristics		Value
EE core dimension A[b]	A	42 mm
EE core dimension B[b]	B	29.5 mm
EE core dimension C[b]	C	12.2 mm
EE core dimension D[b]	D	21.2 mm
EE core dimension E[b]	E	14.8 mm
EE core dimension F[b]	F	20 mm
Effective permeability[b]	μ_e	1781 H/m
Effective length[b]	l_e	97 mm
Effective cross section area[b]	A_e	234 mm^2
Inductance factor[b] (A_L=L/N^2)	A_L	5400 nH/N^2

b. Extracted from [13].

V. Results and Discussions

This section presents the results obtained from the ANSYS Maxwell 2D simulations and the inductance measurements obtained from the transformer prototypes tested in Section IV. Additionally, it contains summary tables with the comparison of these inductance data. The following figures contain the plots of mutual and self-inductance as well as the derived magnetizing and leakage inductances. In both examples, the parameters provided correspond to the primary side. The secondary side inductance values can be seen in [12].

A. Results of Toroidal Core Transformer

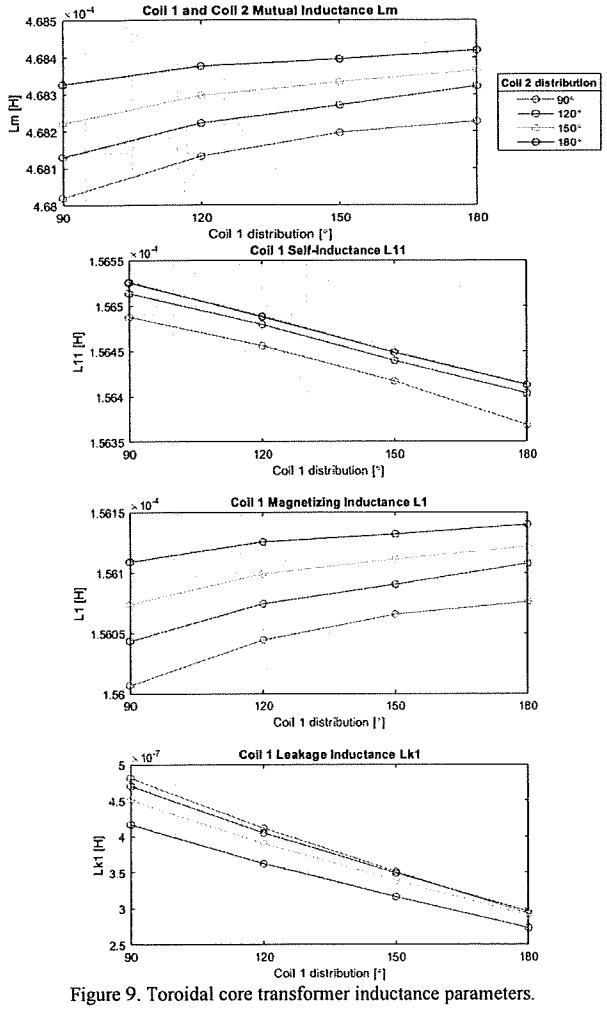

Figure 9. Toroidal core transformer inductance parameters.

The parametric analysis studies the variation in the inductance parameters due to the change in the utilized area of the core where each winding is limited to half the circumference of the core. Fig. 9 presents the inductance profile of this distribution. It can be observed that although the change in the magnitude of the inductance parameters is very small, a clear pattern can be depicted from the mutual and leakage inductance graphs. In this case, the coils start 180° apart with their turns tightly wounded; thus, the leakage inductance of both coils is maximum, and the mutual inductance is minimum due to the lower coupling between the coils in this scenario. Then, when the windings start spreading over the ring core, the leakage considerably decreases because less flux is linked only to the windings' turns. It is interesting to point out that the variation in the inductances is smooth for toroidal distribution where coils do not overlap.

B. Results of EE Core Transformer

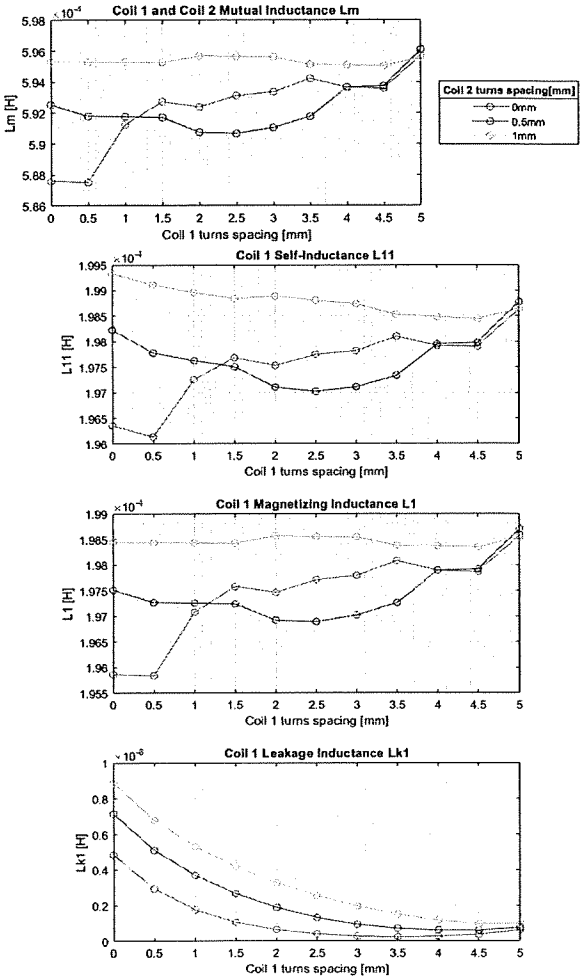

Figure 10. EE core transformer inductance parameters.

Fig. 10 shows the variation of the EE core transformer inductance according to increases in the separation distance of the turns in the windings. In the configuration selected for validation, the leakage inductance of the primary coil decreases as the separation distance between its turns increases. Regarding the mutual and magnetizing inductance, the path that these parameters follow when the spacing in coil 2 is 1 mm is steadier compared with smaller values of spacing, as shown in Fig. 10. The comparison between simulated results and measured values of the toroidal and EE core transformers are presented in Table IV and Table V respectively. The data presented in this chapter correspond to the 2D analysis results from ANSYS Maxwell.